Research Article ISSN 2771-666X

Journal of Advanced Materials Science and Engineering

Bio-Ethanol Production from Cocoyam (*Xanthosoma Sagittifolium*) Peels using Acid Hydrolysis

Nnaji AC[1], Mbah GO[2] and Okorie O[2]*

[1]*Department of Chemical Engineering, Institute of Management and Technology, Enugu State, Nigeria.*

[2]*Department of Chemical Engineering, Enugu State University of Science and Technology, Enugu State, Nigeria.*

***Correspondence:**
Okorie O, Department of Chemical Engineering, Enugu State University of Science and Technology, Enugu State.

Received: 26 Apr 2026; **Accepted:** 28 May 2026; **Published:** 04 Jun 2026

Citation: Nnaji AC, Mbah GO, Okorie O. Bio-Ethanol Production from Cocoyam (*Xanthosoma Sagittifolium*) Peels using Acid Hydrolysis. J Adv Mater Sci Eng. 2026; 6(1): 1-10.

ABSTRACT

This research explored bioethanol production from cocoyam peels using two acid hydrolysis methods—hydrochloric acid (HCl) and sulfuric acid (H_2SO_4) with acid concentrations ranging from 0.1 to 1 M. Before hydrolysis and fermentation, the cocoyam peels were pretreated, and their proximate composition was analyzed. The study investigated how hydrolysis time, pH, temperature, and acid concentration influenced ethanol yield. To optimize sugar yield from acid hydrolysis, the Box-Behnken design within Response Surface Methodology (RSM) was applied. Results showed that sugar yield increased with temperature up to 150°C but declined beyond this point, with a significant decrease observed at 170°C. At 150°C, sugar yield was notably higher than at 130°C and 170°C. The effect of hydrolysis time varied with temperature: below 170°C, maximum sugar yield was reached before 150 minutes, whereas at 170°C, the peak occurred after 60 minutes. Importantly, simple sugar yields from HCl and H_2SO_4 hydrolysis were almost identical. The highest ethanol yield obtained from the acid hydrolysate was 4.55% (v/v). These findings indicate that cocoyam peels, containing approximately 50% carbohydrates, are a promising raw material for bioethanol production.

Keywords

Cocoyam peels, Pretreatment, Acid hydrolysis, Optimization, Bioethanol.

Introduction

Fossil fuels—such as coal, oil, and natural gas—currently supply over 80% of the world's energy consumption. In Nigeria, biomass accounts for approximately 78% of the country's primary energy supply [1-3]. According to the Food and Agriculture Organization Nigeria is the world's largest producer of cocoyam, contributing approximately 3.46 million tons, which accounts for about 37% of global production. China ranks second with 1.64 million tons, followed by Ghana and Cameroon, producing 1.51 million and 1.31 million tons respectively, making them the third- and fourth-largest producers. However, increasing concerns about the depletion of non-renewable resources, the global energy crisis, and the environmental damage caused by fossil fuel use have intensified efforts to explore alternative energy sources. Consequently, there has been growing emphasis on harnessing renewable resources, especially those derived from waste materials, to promote clean energy generation and ensure long-term sustainability [2,4-15]. Clean energy is recognized as a vital component in achieving the United Nations 2030 Sustainable Development Goals (SDGs) and meeting the commitments outlined in the Paris Agreement.

Globally, a vast array of agricultural, plantation, and forestry residues are abundantly available, renewable on an annual basis, and economically feasible for conversion into valuable fuels and chemical products [1,2,16-20]. Recovering energy from these waste streams can substantially reduce the environmental impact of municipal solid waste (MSW) and agricultural residues while providing decentralized, sustainable energy sources for African communities. The total energy potential from waste generated in Africa was estimated at 1,125 petajoules (PJ) in 2012, with

projections increasing to 2,199 PJ by 2025. When considering energy recovery through landfill gas (LFG) and assuming effective waste collection practices, recoverable energy could reach approximately 155 PJ in 2012 and 363 PJ by 2025. The table 1 illustrates that bioethanol yield depends heavily on the type of raw material, the hydrolysis and fermentation methods used, and optimized process parameters such as pH, temperature, substrate concentration, and fermentation time. Cassava and cocoyam peels are prominent feedstocks with promising yields, while the use of microbial consortia and enzymatic hydrolysis appears effective in enhancing ethanol production. The variation in yields also suggests opportunities for further optimization and scale-up depending on the feedstock and technology employed.

Acid hydrolysis is among the most commonly used chemical methods for breaking down lignocellulosic biomass. It can serve either as a pretreatment step prior to enzymatic hydrolysis or as the primary technique for converting lignocellulose into fermentable sugars. Many commercial bioethanol production processes currently utilize acid pretreatment because it achieves high reaction rates and significantly improves cellulose hydrolysis efficiency [24]. A major advantage of acid hydrolysis is its high-yield conversion of xylan into xylose, which is crucial for the economic viability of ethanol production from lignocellulosic feedstocks [25,26].

As biomass hydrolysis and fermentation technologies progress toward commercial-scale adoption, innovations in product recovery methods will become increasingly important. Bioethanol produced via fermentation requires separation and purification typically through distillation to isolate ethanol from water. Therefore, developing and applying efficient technologies for the recovery and reuse of this abundant, energy-rich waste resource is essential to maximize resource utilization and enhance the sustainability of bioethanol production systems.

Material and Methods

Sample Collection

50kg of cocoyam (Colocasia esculenta) peels were collected from different homes at Emene in Enugu East L.G.A, Enugu State of Nigeria. The sample was gathered, cleaned, washed thoroughly with distilled water and sun dried for two weeks. The sample was milled into powdered form using an electric grinder and sieved to a fine particle size of 250$^{\mu m}$, sun dried again for a week and then packaged in a well labeled airtight containers for analyses.

Acidic Hydrolysis of the Cocoyam Peels

The cocoyam peels were acid hydrolyzed with varying amounts of hydrochloric and sulfuric acids. 1g of the pretreated peels was weighed into separate 100ml conical flasks for acidic hydrolysis. The flasks each held 50ml of various acid concentrations ranging from 0.1 to 1.0M. The flasks were wrapped in aluminum foil and put in an electric oven set to a specific temperature. The duration of the hydrolysis ranged from 10 to 90 minutes. The flasks were then taken out of the oven and filtered with a vacuum filter. To obtain the hydrolyzate, the filtrates were neutralized with a 3M NaOH solution. The yield of simple sugars was determined using Equation 3.3 and the concentration of simple sugar in the neutralized solutions was analyzed using DNS reagent [27].

Fermentation Experiment

The acidic hydrolyzates were fermented with commercial saccharomyces cerevisae purchased from the market. Fermentation was done in 100mL plastic bottles containing 20ml of the hydrolyzate. 1M NaOH and 1M HCl were used to change the pH of the hydrolyzate, and the yeast weight ranged from 0.1 to 0.3g. The containers were vigorously shaken for 30 minutes to ensure proper dissolution of the yeast cells into the hydrolyzate, and then covered with cotton wools to allow CO_2 to escape as a bye-product of fermentation. Depending on the design run, the containers were left to stand for 3 days, after which the mixture was filtered using a vacuum filter. A basic distillation setup was used to distill the fermentation filtrate. A specific gravity/ethanol meter was used to calculate the consistency of the ethanol in the distillate (DA-130N).

Analysis of Simple Sugars

The DNS method (Dinitrosalicylic acid) was used to build a standard

Table 1: Summary of bio-ethanol yields from different agricultural wastes.

Authors	Raw material used	Method	Process conditions	Optimum Bio-ethanol yield
Femi et al., [21]	500g of Cassava peels	Developed Percolation reactor		118mL
Nnaji et al., [4]	100g of Cocoyam peels	Enzymatic hydrolysis		7.15%(v/v)
Adegunloye and Udenze [9]	60g of Cocoyam peels	Enzymatic hydrolysis	Fermentation (7days), pH(5)	5.65g/100mL
Efeovbokhan et al., [22]	Hybrid cassava pulp and peel	Microbial and acid hydrolysis		54.8% and 33.1% respectively
Mustafa et al., [8]	20g of cassava peels	Acid hydrolysis	Temperature (28°C), pH (4.55), substrate concentration (10%), period of fermentation (4 days)	37.35g/mL
Olawale et al., [5]	Watermelon peels	Aspergillus niger and Saccharoymces cerevisiae	Temperature(30°C, pH(6), 4% g/L substrate, 5 days of fermentation period	57g/L
Amadi et al., [23]	Cocoyam peels, leaves and stalks	Microbial enzymatic hydrolysis	pH(5), Carbon concentration of 5%(peel, stalk) and 4% (leaf)	Bioethanol from the peels (0.21%), leaves (0.38%), combined substrates(0.28%)

glucose calibration curve [28]. By dissolving the equivalent amount of glucose powder in distilled water, standard glucose solutions of 0.2, 0.4, 0.6, 0.8, 1.0, and 1.2 percents were made. The basic calibration curve was created by developing standard solutions with DNS reagent and recording the absorbance at 540nm in a UV spectrophotometer. In a one-liter volumetric flask, 10 grams of DNS, 0.5 grams of sodium sulfite, and 10 grams of sodium hydroxide were mixed with water to make the DNS reagent. 3ml of each of the standard solutions is measured in test tubes to establish the standards with DNS. After that, 3ml of DNS reagent was applied to each tube, which was then covered with aluminum foil. Following that, the color was created by boiling the tubes for 10 minutes. After allowing the tubes to cool, the absorbance was measured at 540nm. A standard equation was obtained by plotting the absorbance against the glucose concentration. To determine the concentration of any sample, 3mL of the sample was heated with 3mL of DNS reagent, and the absorbance of the color produced from the sample was used to measure the sample's simple sugar concentration.

Kinetics of the Acidic Hydrolysis

Equation 1 depicts the hydrolysis reaction, while equations 2 and 3 depict the rate equations that go along with it.

Polymer K_1 Monomer K_2 Decomposition -- (1)

$$\frac{dP}{dt} = -K_1[P] \quad - \quad - \quad - \quad - \quad - \quad (2)$$

$$\frac{dM}{dt} = K_1[P] - K_2[M] \quad - \quad - \quad - \quad - \quad (3)$$

where

K_1 and K_2 are the rate constants for the formation and decomposition of the simple sugars respectively, P is the polymer (Cellulose) concentration and M is the monomer (simple sugar) concentrations.

The equation was constructed based on the assumption that the reactions were pseudo homogeneous, despite the fact that they were heterogeneous in principle, involving solid phase biomass and liquid phase acid catalysis. With the assumption that the biomass as obtained contains no simple sugar, the differential equations were combined and solved in terms of monomer concentration, and the result is shown in Equation 4 [27].

$$M = \left[\frac{K_1 P_0}{K_2 - K_1}\right](e^{-K_1 t} - e^{-K_2 t}) \quad - \quad - \quad - \quad (4)$$

Using Microsoft Excel Solver, the kinetics equation was solved to find the best K_1 and K_2 values. The aim was to reduce the absolute error between the real data and the model as much as possible, with the rate constants' values not being allowed to be negative.

Optimization of the Acidic Hydrolysis

Table 1 presents the Box-Behnken design matrix used for the Response Surface Methodology (RSM). In this design, acid concentration served as the response variable, while three numerical factors—time, temperature, and acid concentration—were considered. The Box-Behnken design was specifically selected to prevent the inclusion of impractical or negative experimental points, thereby ensuring all conditions were feasible for implementation.

Table 1: Box-Behnken of Response Surface Methodology Design Matrix for Acidic Hydrolysis.

STD	Run	Time(min)	Temp(°C)	Acid Conc. (M)	Sugar yield (%)
12	1	50	170	1	
2	2	90	130	0.55	
17	3	50	150	0.55	
5	4	10	150	0.1	
14	5	50	150	0.55	
9	6	50	130	0.1	
4	7	90	170	0.55	
8	8	90	150	1	
7	9	10	150	1	
6	10	90	150	0.1	
16	11	50	150	0.55	
10	12	50	170	0.1	
3	13	10	170	0.55	
15	14	50	150	0.55	
1	15	10	130	0.55	
11	16	50	130	1	
13	17	50	150	0.55	

Results and Discussion

Acidic Hydrolysis of Cocoyam Peels

The Effects of Time and Temperature on Acidic Hydrolysis of Cocoyam Peels

Figures 1 to 3 illustrate the effects of time and temperature on the acid hydrolysis of cocoyam peels. The sugar yield increased with rising temperature, reaching its peak at 150°C. However, a decline in yield was observed when the temperature reached 170°C, indicating an optimal temperature range for hydrolysis efficiency. Specifically, the yield at 150°C was higher compared to those at 130°C and 170°C. The influence of hydrolysis time was found to be temperature-dependent. At temperatures below 170°C, maximum sugar yield was achieved before 150 minutes, whereas at 170°C, the peak occurred much earlier—after just 60 minutes. Additionally, it is noteworthy that the simple sugar yields obtained from hydrochloric acid (HCl) hydrolysis were nearly identical to those produced using sulfuric acid (H_2SO_4), suggesting comparable effectiveness between the two acids under similar conditions.

Kinetics of Acidic Hydrolysis of Cocoyam Peels

The kinetic constants K_1 (sugar formation) and K_2 (sugar decomposition) were calculated using Microsoft Excel Solver, and their values were plotted against temperature in Figures 4 to 6. The results show that as temperature increased, the value of K_1 also increased, indicating an accelerated rate of sugar formation at higher temperatures. Notably, for sulfuric acid (H_2SO_4), the sugar formation rate at 150°C was nearly the same as at 130°C. In contrast, hydrochloric acid (HCl) exhibited a significantly higher sugar

formation rate at 150°C compared to 130°C, suggesting greater temperature sensitivity. Conversely, the sugar decomposition rate constant K_2 decreased with increasing temperature, indicating a slower degradation of sugars at elevated temperatures.

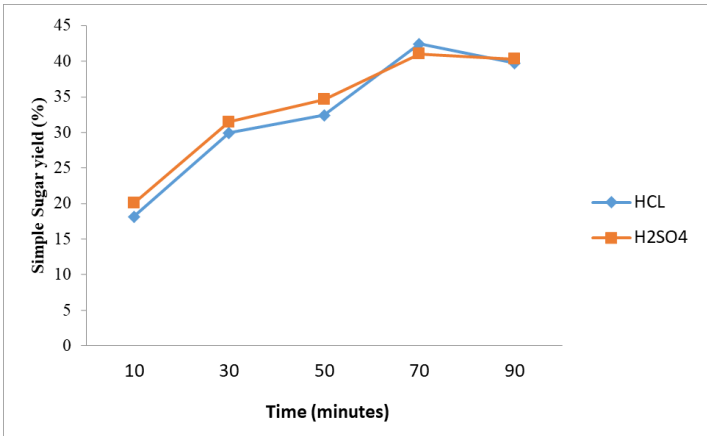

Figure 1: Effect of time (minutes) on simple sugar yield at temperature of 130°C.

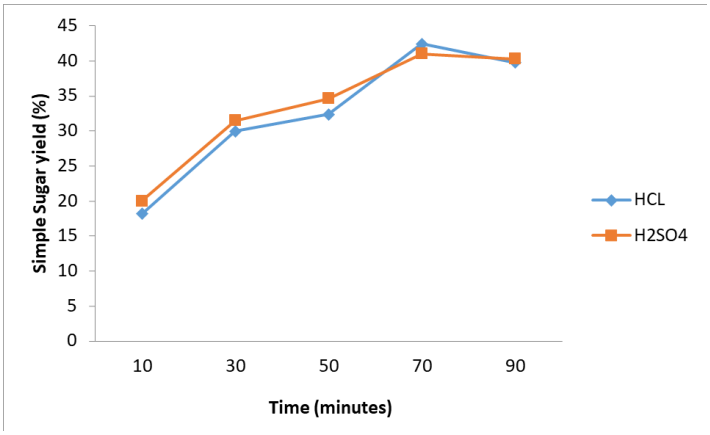

Figure 2: Effect of time (minutes) on simple sugar yield at temperature of 150°C.

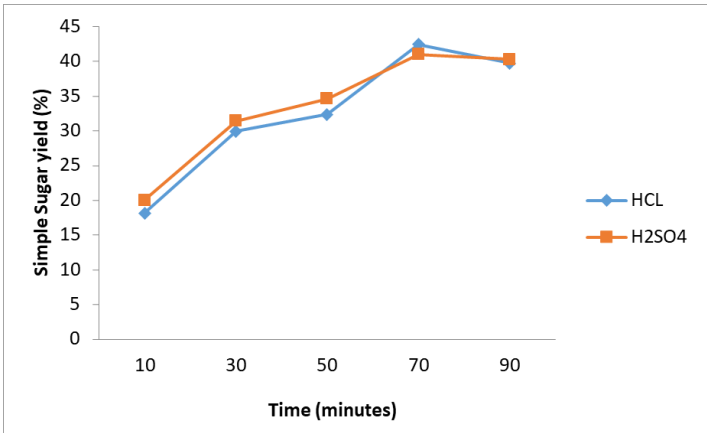

Figure 3: Effect of time (minutes) on simple sugar yield at temperature of 170°C.

Overall, the rate of sugar formation consistently exceeded the rate of sugar decomposition across all tested conditions, highlighting favorable kinetics for sugar accumulation under these hydrolysis conditions.

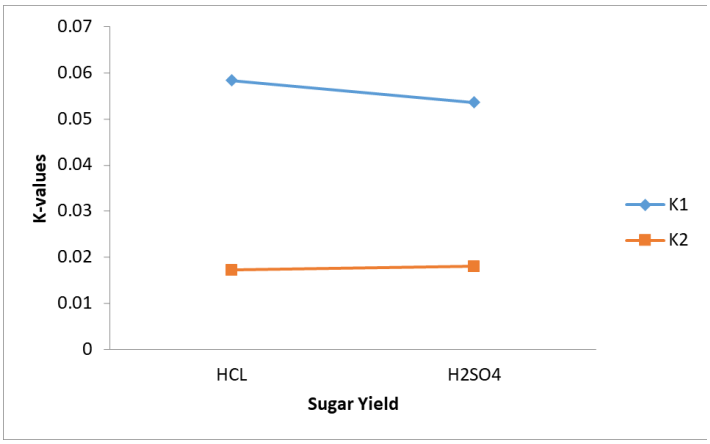

Figure 4: Kinetics Constants with respect to temperature (130°C).

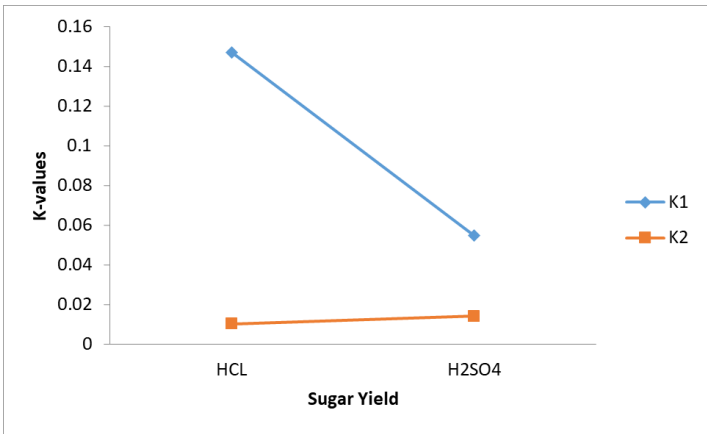

Figure 5: Kinetics Constants with respect to temperature (150°C).

Effect of Acid Concentration on Acidic Hydrolysis of Cocoyam peels

Figures 7 to 9 illustrate the impact of acid concentration on simple sugar yield. The data reveal that sugar yields were lowest at 0.1 M acid concentration for both hydrochloric acid (HCl) and sulfuric acid (H_2SO_4). Higher yields were achieved at 0.5 M and 1.0 M concentrations; however, the yield at 0.5 M exceeded that at 1.0 M. This suggests that sugar production declines beyond the optimal concentration, likely due to saturation effects or sugar degradation. This preliminary analysis indicates that the optimal acid concentration for maximizing simple sugar yield is approximately 0.5 M. Additionally, the difference in sugar yields between HCl and H_2SO_4 at the same concentrations was minimal, demonstrating that both acids are similarly effective under these conditions.

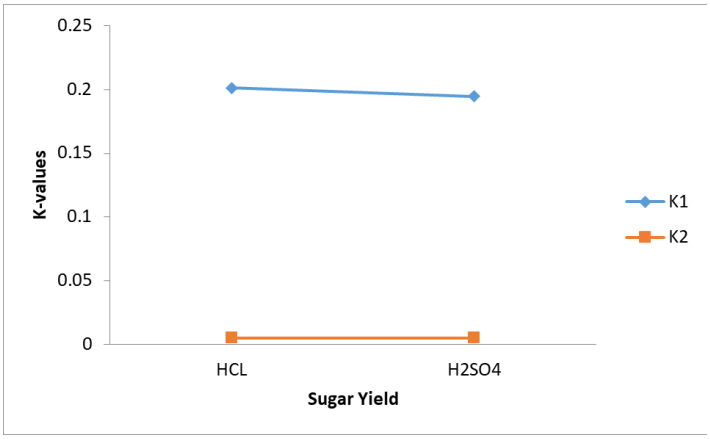

Figure 6: Kinetics Constants with respect to temperature (170°C).

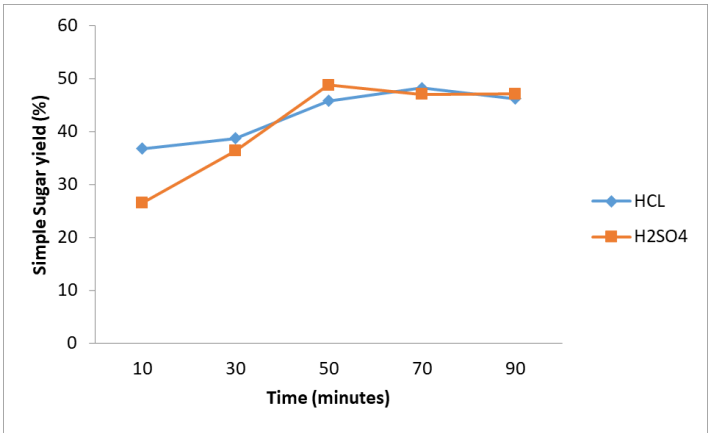

Figure 8: Effect of acid concentrations on simple sugar yield at 0.5M.

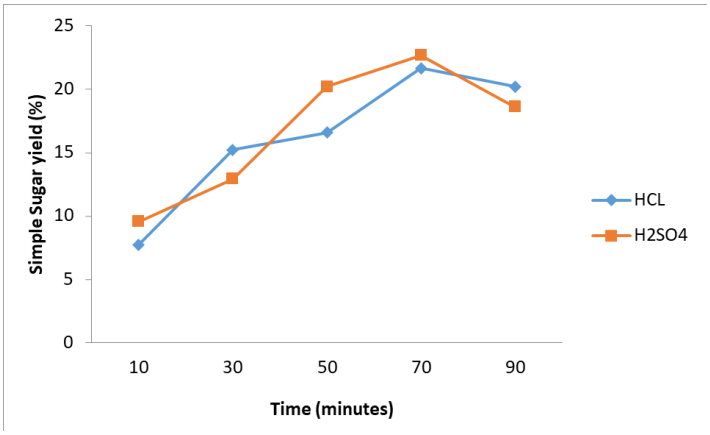

Figure 7: Effect of acid concentrations on simple sugar yield at 0.1M.

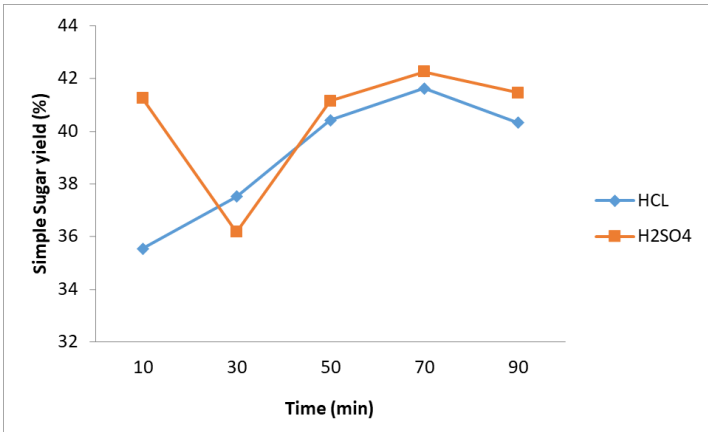

Figure 9: Effect of acid concentrations on simple sugar yield at 1.0M.

Table 2: ANOVA table for Differences among yield from HCl and H_2SO_4.

0.1M Acid Solution	Source of Variation	SS	Df	MS	F	P-value	F crit
	Between Groups	0.665939	1	0.665939	0.022599	0.884225	5.317655
	Within Groups	235.7386	8	29.46732			
	Total	236.4045	9				
0.5M Acid Solution	Source of Variation	SS	Df	MS	F	P-value	F crit
	Between Groups	9.903506	1	9.903506	0.168827	0.691942	5.317655
	Within Groups	469.2853	8	58.66066			
	Total	479.1888	9				
1.0M Acid Solution	Source of Variation	SS	Df	MS	F	P-value	F crit
	Between Groups	4.723076	1	4.723076	0.77876	0.403257	5.317655
	Within Groups	48.51892	8	6.064865			
	Total	53.24199	9				

The Differences between yields from HCl and H_2SO_4

A one-way Analysis of Variance (ANOVA) was performed using Microsoft Excel to assess the statistical differences in simple sugar yields resulting from hydrochloric acid (HCl) and sulfuric acid (H_2SO_4) hydrolysis. As summarized in Table 2, the results show that at a 0.05 significance level, there is no statistically significant difference between the sugar yields produced by the two acids. This conclusion is supported by calculated F-statistics being lower than the critical F-value and p-values exceeding the 0.05 threshold. These findings indicate that the type of acid whether HCl or H_2SO_4 does not significantly affect sugar yield across the tested concentrations. Therefore, either acid can be effectively used for hydrolysis, as their performance differences are not statistically significant. In statistical terms, the null hypothesis stating no difference in sugar yields between HCl and H_2SO_4 could not be rejected.

Optimization of Acidic Hydrolysis of Cocoyam Peels

The Box-Behnken Design (BBD) of Response Surface Methodology (RSM) was utilized to optimize simple sugar yield

during acid hydrolysis. Table 3 displays the design matrix alongside the corresponding sugar yields obtained using hydrochloric acid (HCl). Since statistical analysis showed no significant difference in sugar yields between HCl and sulfuric acid (H_2SO_4), only HCl was chosen for the optimization study. Seventeen experimental runs were performed, and the resulting data were analyzed using Design Expert software. Based on the observed response patterns, the software recommended a quadratic model for further evaluation. The model's adequacy and the significance of its terms were assessed through Analysis of Variance (ANOVA). With the model demonstrating a strong fit and statistical validity, sugar yield optimization was carried out using the quadratic model.

Table 3: Design Matrix with Response for Acidic Hydrolysis.

Std	Run	Time (minutes)	Temp °C	Acid Conc (M)	% Yield
12	1	50	170	1	42
2	2	90	130	0.55	30.45
17	3	50	150	0.55	47
5	4	10	150	0.1	7.7
14	5	50	150	0.55	46
9	6	50	130	0.1	22
4	7	90	170	0.55	39.74
8	8	90	150	1	40.3
7	9	10	150	1	35.5
6	10	90	150	0.1	20.2
16	11	50	150	0.55	49
10	12	50	170	0.1	34
3	13	10	170	0.55	28.3
15	14	50	150	0.55	45.8
1	15	10	130	0.55	18.15
11	16	50	130	1	35
13	17	50	150	0.55	48

Analysis of Variance (ANOVA) for Acidic Hydrolysis

Table 4 shows the ANOVA table for the quadratic model of simple sugar yield as a function of time, temperature, and acid concentration. The model and key factor effects p-values were less than 0.05 at the significance stage. This verified that the quadratic model fit the system well and that the factors were indeed important for acidic hydrolysis. They had a significant impact on the overall yields of simple sugars due to the squared effects' p-values all less than 0.05. The two-factor effects, on the other hand, were greater than 0.05 and not significant at the 0.05 level. This means that one factor's effect is independent of the level of another.

Model Equation and Graphs for Acidic Hydrolysis

In acidic hydrolysis, Equation 5 shows the quadratic model equation for the yield of simple sugars as a function of time, temperature, and acid concentration. According to the ANOVA, the quadratic equation only contains important expressions. Fig. 10 to Fig. 12 display the 3D model graphs. The optimum yield could be found in the center of the time/temperature, time/acid concentration, and temperature/acid concentration spaces at constant acid concentration and varying temperature and time.

Table 4: The ANOVA for Acidic Hydrolysis.

	Sum of		Mean	F		
Source	Squares	DF	Square	Value	Prob > F	
A	210.5352	1	210.5352	14.31216	0.0069	
B	184.7042	1	184.7042	12.55617	0.0094	
C	593.4013	1	593.4013	40.33934	0.0004	
A^2	675.1112	1	675.1112	45.89397	0.0003	
B^2	119.9533	1	119.9533	8.15441	0.0245	
C^2	309.4221	1	309.4221	21.03448	0.0025	
AB	0.1849	1	0.1849	0.012569	0.9139	
AC	14.8225	1	14.8225	1.007632	0.3489	
BC	6.25	1	6.25	0.424874	0.5353	
Residual	102.9717	7	14.71024			
Lack of Fit	95.65965	3	31.88655	17.44341	0.0092	Significant
Pure Error	7.312	4	1.828			
Cor Total	2328.273	16				

$$\text{Yield (\%)} = -355.06 + 1.02 \times \text{Time (min)} + 4.33 \times \text{Temp (°C)} + 91.89 \times \text{Acid Conc (Molar)} - 0.01 \times \text{Time}^2 - 0.01 \times \text{Temp}^2 - 42.33 \times \text{Acid Conc}^2 \quad \text{---------- (5)}$$

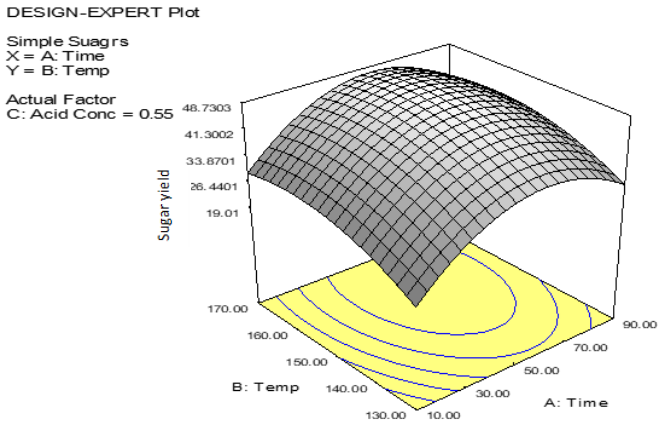

Figure 10: 3D Graph of Time and Temperature against simple sugars yield.

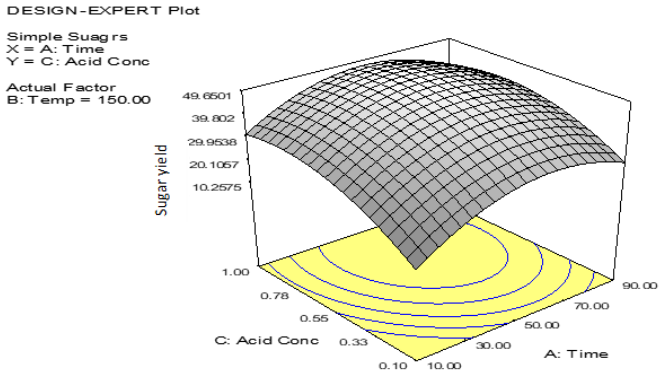

Figure 11: 3D Graph of Time and Acid Concentration against Simple Sugars Yield.

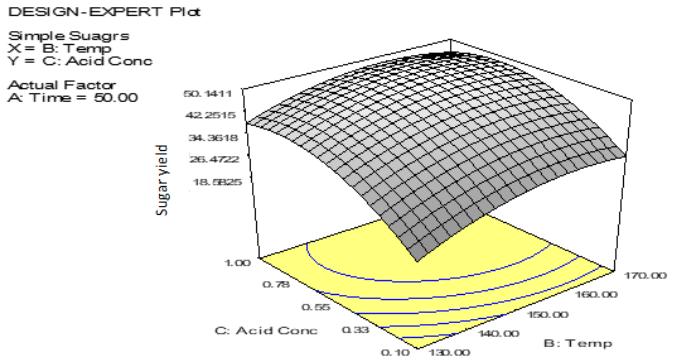

Figure 12: 3D Graph of Temperature and Acid Concentration against Simple Sugars Yield.

Numerical Optimum Solution for Acidic Hydrolysis

Table 5 shows the theoretical and numerical optimum solution for acidic hydrolysis of cocoyam peels. The actual yield was obtained by hydrolyzing for 56 minutes at 150°C with 0.78M HCl, and the yield of simple sugars was 51 percent under these conditions. This finding is reasonable in comparison to the theoretical value of 49.8%. As a result, the optimum solution for time, temperature, acid concentration, and simple sugars yield was verified at 56 minutes, 150°C, 0.78M, and 51%, respectively.

Table 5: The Numerical Optimum Solution for Acidic Hydrolysis.

Time (day)	Temp (°C)	Acid Conc (M)	Yield (%)	Actual (%)
56.22	150.77	0.78	49.8	51

Ethanol Fermentation Results

Effects of Process Parameters on Ethanol Yield

Figures 13-15 depict the effects of time, pH, and enzyme dosage on ethanol yield at constant temperature. The yields of ethanol increased over time and remained steady after four days of fermentation. Ethanol yields peaked around pH 6 and 7, after which they began to decline at higher pH. The effects of enzyme dosage were so strong that the yields from both acid and alkaline hydrolyzates differed almost equally. The yields also peaked around the dosage of 4mL/20mL mixtures, after which they began to decline.

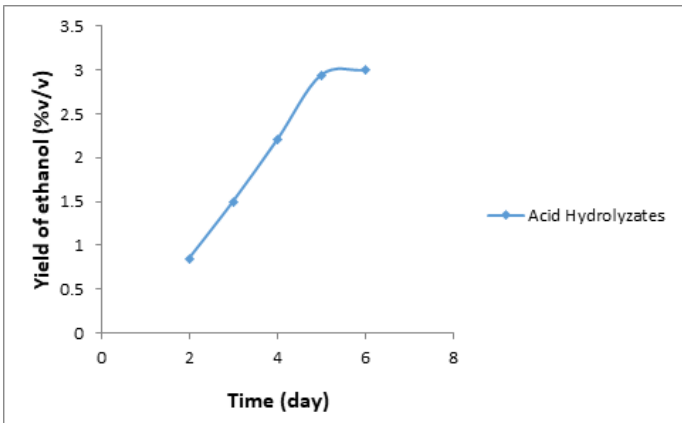

Figure 13: Effect of time on Ethanol Yield.

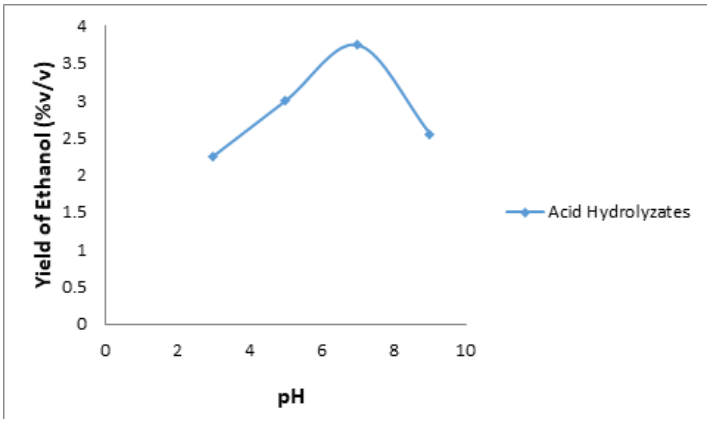

Figure 14: Effect of pH on Ethanol Yield.

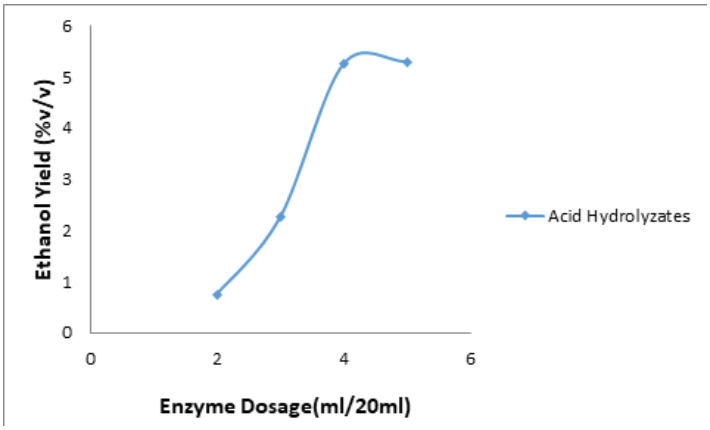

Figure 15: Effect of Enzyme Dosage on Ethanol Yield.

Kinetics of Ethanol Fermentation

The kinetics of the fermentation process was investigated using the Michaelis Menten model as shown in Table 6. Although the regression coefficients (R^2) were similar to 1.0, the data with acid hydrolyzate matched the Michaelis Menten model very well and the kinetics constant for acid hydrolyzate fermentation was higher.

Table 6: Kinetics Parameters for the Fermentation Reactions.

Substrate	V_ml	K_m	R^2
Acid Hydrolyzate	41.322	202.865	0.835

Optimization of Fermentation Process

Table 7 presents the Box-Behnken design matrix along with the corresponding responses for acid hydrolyzate fermentation. The experimental data were analyzed using Design Expert software, which identified quadratic models as the most suitable for describing the fermentation responses. The adequacy and significance of these models were subsequently validated through Analysis of Variance (ANOVA), as summarized in Table 8.

Table 7: Design matrix with responses of ethanol yields from Acid Hydrolyzate.

Std	Run	Time (day)	pH	Yeast Dosage (g/20mL)	Acid Hydrolyzate Ethanol (%v/v)
1	15	2	3	1.5	1.5
2	16	6	3	1.5	3.2
3	17	2	9	1.5	2.1
4	1	6	9	1.5	3.9
5	13	2	6	1	3.4
6	9	6	6	1	4.3
7	8	2	6	2	3.8
8	10	6	6	2	4.6
9	5	4	3	1	3.2
10	6	4	9	1	3.8
11	12	4	3	2	3.7
12	4	4	9	2	4.4
13	14	4	6	1.5	4.5
14	7	4	6	1.5	4.7
15	2	4	6	1.5	4.3
16	11	4	6	1.5	4.5
17	3	4	6	1.5	4.6

The ANOVA of the Quadratic Models of the Ethanol Fermentation

The quadratic model and the main effects of the key factors—time (A), pH (B), and yeast dosage (C)—were evaluated using Analysis of Variance (ANOVA), as shown in Table 8. At the 0.05 significance level, time and pH were found to have statistically significant effects on the fermentation of acid hydrolyzates, as their p-values were below 0.05. However, the p-value for yeast dosage (C), presented in Table 8, exceeded 0.05, indicating that yeast dosage did not have a statistically significant impact on ethanol yield within the experimental range. Furthermore, the squared terms of time (A2A^2A2) and pH (B2B^2B2) were statistically significant, while the squared term for yeast dosage (C2C^2C2) was not. None of the two-factor interaction effects (AB, AC, and BC) were significant at the 0.05 level, suggesting that interactions between these variables did not meaningfully influence the fermentation outcome. Additionally, the p-values for lack of fit were greater than 0.05, indicating that the lack of fit was not statistically significant. This suggests that the quadratic model adequately fits the experimental data and there was no substantial deviation requiring concern.

Table 8: The ANOVA Table of Quadratic Model for Fermentation of Acid Hydrolyzate.

Source	Sum of Squares	DF	Mean Square	F Value	Prob > F
A	3.38	1	3.38	46.120858	0.0003
B	0.845	1	0.845	11.530214	0.0115
C	0.405	1	0.405	5.5263158	0.051
A^2	2.677921	1	2.677921	36.540833	0.0005
B^2	4.620026	1	4.620026	63.041295	< 0.0001
C^2	0.385289	1	0.385289	5.2573612	0.0556
AB	0.0025	1	0.0025	0.0341131	0.8587
AC	0.0025	1	0.0025	0.0341131	0.8587
BC	0.0025	1	0.0025	0.0341131	0.8587
Residual	0.513	7	0.073286		
Lack of Fit	0.425	3	0.141667	6.4393939	0.0519
Pure Error	0.088	4	0.022		
*Cor Total	13.00941	16			

The Quadratic Model Equations of the Fermentation Process

Equation 6 for fermentation of acid hydrolyzate of cocoyam peels, demonstrate the mathematical model equations for ethanol yield as a function of time, pH, and yeast dosage. The non-significant terms are not present in the model equations, as shown by the ANOVA table.

Ethanol Yield % = -2.66 + 1.93×Time + 1.46×pH - 3.18×Enzyme Dosage - 0.199×$Time^2$ -0.12×pH^2 + 1.21×$Enzyme\ Dosage^2$ ……(6)

The 3D Graph of time and pH against the ethanol yield

Ethanol yield from acid hydrolyzates was significantly influenced by both fermentation time and pH. As illustrated in the 3D surface plots in Figure 16, the optimal ethanol yield under constant temperature and yeast dosage was observed within the design space at mid-range pH values and extended fermentation times. This observation aligns with the results of the ANOVA analysis, which confirmed that both time and pH had statistically significant effects on ethanol production. Notably, their influence remained significant even at the 0.01 level, with corresponding p-values less than 0.01, underscoring their critical role in optimizing fermentation efficiency.

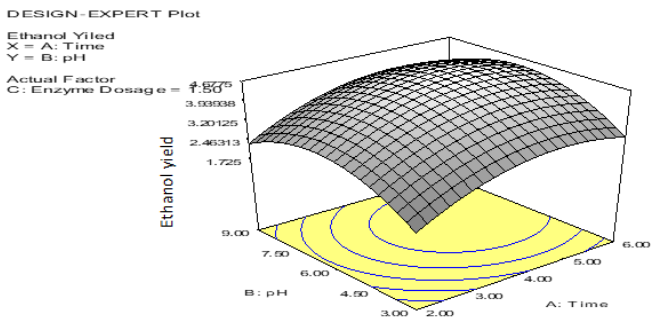

Figure 16: 3D Graph of Time, pH and Ethanol Yield for Fermentation of the Acid Hydrolyzates.

The 3D graph of Time and Yeast Dosage against Ethanol Yield

Figure 17 presents 3D surface plots illustrating the relationship between fermentation time and enzyme dosage on ethanol yields from acid hydrolyzates. It is evident that variations in time had a more pronounced effect on ethanol yield compared to changes in enzyme dosage. The optimum ethanol yield—under constant temperature and pH conditions—was observed near the upper end of the time range. This finding is supported by the ANOVA results, which show that the p-values associated with enzyme dosage were slightly above the 0.05 significance level. This indicates that enzyme dosage had a relatively minor effect on ethanol yield within the tested range, whereas time remained a more critical

factor in optimizing fermentation performance.

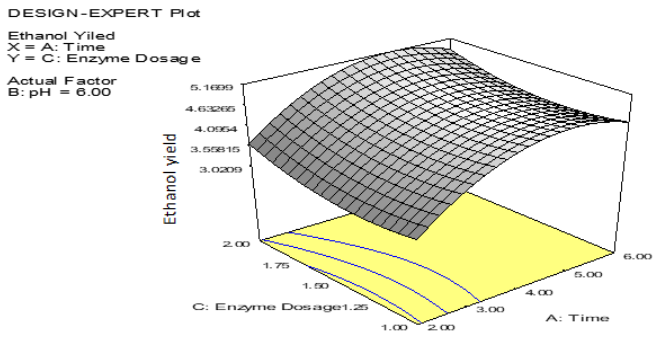

Figure 17: 3D Graph of Time, Yeast Dosage and Ethanol Yield for Fermentation of the Acid Hydrolyzates.

The 3D Graph of pH and Yeast Dosage against Ethanol Yield

Figure 18 illustrates a 3D surface plot depicting the effects of pH and enzyme dosage on ethanol yield from acid hydrolyzate. The graph clearly indicates that pH had a more significant impact on ethanol yield compared to enzyme dosage. At constant fermentation time and temperature, the optimal ethanol yield was observed around the mid-range of the pH values, highlighting the critical role of pH in optimizing the fermentation process.

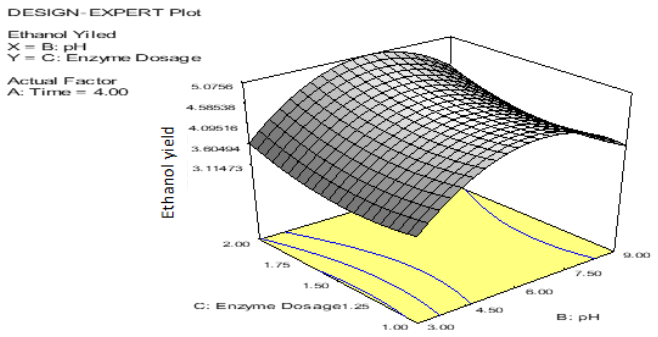

Figure 18: The 3D Graph of pH, Yeast Dosage and Ethanol yield for Fermentation of the Acid Hydrolyzates.

The Numerical Optimum Solutions of Ethanol Yields for the Fermentation of Acid Hydrolyzate of Cocoyam Peels

Table 9 shows the numerical optimum solutions for ethanol yield as a function of time, pH, and yeast dosage in the fermentation of acid hydrolyzate of cocoyam peels. Fermentation of acid hydrolyzate of cocoyam peels for 5 days at pH 6.9 and yeast dosage of 1.7g/20ml was used to confirm the optimum ethanol yield. The yield of ethanol was 4.55 percent (v/v). The real yield was 4.76 percent (v/v), which was equivalent to the theoretical yield. As a result, the optimum ethanol yields for acid hydrolyzate was 4.55 percent (v/v).

Table 9: The Optimum Numerical Solution for Fermentation of Acid Hydrolyzate of Cocoyam peels.

Substrate	Time (day)	pH	Yeast Dosage (g/20mL)	Ethanol (%v/v)	Actual Ethanol (%v/v)
Acid hydrolyzate	5	6.9	1.7	4.76	4.55

Characterization of Ethanol Produced

Table 10 provides a comparison between the refractive indices of ethanol produced from cocoyam peel hydrolysates and standard ethanol samples at equivalent concentrations. The ethanol sample derived from acid hydrolysates exhibited a refractive index of 1.3355 at a concentration of 4.55% (v/v), which is very close to the standard ethanol refractive index of 1.3357 at the same concentration. Additionally, a standard ethanol sample with a higher concentration of 7.15% (v/v) had a refractive index of 1.3373, illustrating the expected trend that refractive index increases with ethanol concentration. This high degree of similarity in refractive indices—differing by only 0.0002 units—confirms that the ethanol produced from cocoyam peels shares the same optical properties as pure ethanol, thereby validating the purity and identity of the bioethanol produced. This outcome serves as an effective qualitative confirmation of successful ethanol production via acid hydrolysis.

Furthermore, the measured ethanol yield of 7.15% (v/v) closely matches the theoretical yield of 7.04% (v/v), reflecting a high process efficiency and minimal loss during hydrolysis and fermentation. However, the study identifies 4.55% (v/v) as the optimum ethanol yield specifically obtained from the acid hydrolysate, which likely represents the highest consistent yield under optimized conditions such as temperature, time, pH, and acid concentration.

Table 10: The Refractive Indices of Ethanol Produced.

	Ethanol (%v/v)	Refractive Index
Ethanol from Acid Hydrolyzates	4.55	1.3355
Standard Ethanol	4.55	1.3357
Standard Ethanol	7.15	1.3373

Conclusion

In summary, this study confirms the viability of cocoyam peels as a sustainable and efficient feedstock for bioethanol production, primarily due to their high carbohydrate content and abundant availability. The use of hydrochloric and sulfuric acid in acid hydrolysis yielded comparable results, and process optimization via Response Surface Methodology (RSM) identified 150°C as the optimal temperature for maximizing sugar release. Despite a decline in sugar yield at excessively high temperatures, the process successfully produced a significant ethanol yield of 4.55% (v/v). Compared to other biomass sources, tuber waste such as cocoyam peels presents a more accessible and cost-effective option, making it well-suited for large-scale bioethanol production. Beyond its technical feasibility, the integration of bioethanol into the transportation sector offers broader environmental and socioeconomic benefits, including reduced greenhouse gas

emissions, enhanced energy security, and opportunities for rural development. As global energy strategies increasingly prioritize renewable alternatives, the valorization of tuber crop waste for bioethanol stands out as a practical and promising pathway toward a cleaner, more sustainable future.

References

1. Agbro EB, Ogie NA. A comprehensive review of biomass resources and biofuel production potential in Nigeria. Res J in Eng App Sci. 2012; 1: 149-155.
2. Kuye AO, Edeh I. Production of bio-oil from biomass using fast pyrolysis: A critical review. J of Mine Res. 2013; 1: 1-19.
3. Ana GREE, Sokan-Adeaga AA. Bio-Ethanol Yield from Selected Lignocellulosic Wastes. Inter J of Sustainable Green Eng. 2015; 4: 141-149.
4. Nnaji AC, Mbah GO, Onoh MI, et al. Bio-ethanol production from cocoyam peels using enzymatic hydrolysis. J of Mate Sci Re Revi. 2021; 8: 13-28.
5. Olawale OE, Olusola-Makinde O, Oladunmoye MK. Synergistic antibacterial potentials of Ocimum gratissimum, honey and ciprofloxacin against some multiple antibiotic-resistant bacteria isolated from stool samples. Walailak J of Sci Tech. 2021; 18: 9192.
6. Vaish B, Singh P, Kothari R, et al. The potential of bioenergy production from marginalized lands and its effect on climate change. Climate Change Environ Sustain. 2016; 4: 7-13.
7. Vaish B, Srivastava V, Singh PK, et al. Energy and nutrient recovery from agro-wastes: Rethinking their potential possibilities. Environ Eng Res. 2020; 25: 623-637.
8. Mustafa HM, Salihu D, Bashir A, et al. Bio-ethanol production from cassava Manihot esculenta waste peels using acid hydrolysis and fermentation process. Sci Wor J. 2019; 14: 45-50.
9. Adegunloye DV, Udenze DO. Effect of fermentation on production of bioethanol from peels of cocoyam using Aspergillus niger and Saccharomyces cerevisiae. J of Adva in Micro. 2017; 4: 1-8.
10. Supramono D, Lusiani S. Improvement of bio-oil yield and quality in co-pyrolysis of corncobs and high density polyethylene in a fixed bed reactor at low heating rate. Mater Sci Eng. 2016; 162: 012011.
11. Sutrisno B, Hidayat A. Upgrading of bio-oil from the pyrolysis of biomass over the rice husk ash catalysts. Mater Sci Eng. 2016; 162: 012014.
12. Srivastava V, Ismail SA, Singh P, et al. Urban solid waste management in the developing world with emphasis on India: challenges and opportunities. Rev Environ Sci Bio. 2015; 14: 317-337.
13. Bridgwater AV, Meier D, Radlein D. An overview of fast pyrolysis of biomass. Organic geochemistry. 1999; 30: 1479-1493.
14. Sivakumar G, Vail DR, Xu J, et al. Bioethanol and biodiesel: Alternative liquid fuels for future generations. Engi in Life Sci. 2010; 10: 8-18.
15. El Harchi M, Fakihi Kachkach FZ, El Mtili N. Optimization of thermal acid hydrolysis for bioethanol production from Ulva rigida with yeast Pachysolen tannophilus. South African J of Botany. 2018; 115: 161-169.
16. Demirbas A. Competitive liquid biofuels from biomass. App Ene. 2011; 88: 17-28.
17. Ohunakin OS. Energy Utilization and Renewable Energy Sources in Nigeria. J of Eng Appl Sci. 2010; 5: 171-177.
18. Okorie O, Edem UB, Edeh I, et al. Pretreatment of rubber tapping Heava brasiliensis and achi mkpuru Gossweilerodendron balsamiferum Hardwood sawdust for bio-oil production: Drying and particle size characteristics at different temperatures. Appl Sci. 2015; 5: 171-177.
19. Edem UB, Okorie O, Edeh I, et al. Drying and particle size characteristics of Danta Nesogordonia papavereria and hard cross Vitex doniana Wood Sawdusts at Different Temperatures. J of Alternate Ene Sources Techn. 2016; 7: 30-38.
20. Juliet B, Vasilije M, Philip L. Biomass resources and biofuels potential for the production of transportation fuels in Nigeria. Renew Sustai Ene Revi. 2016; 63: 172-192.
21. Femi TI, Ahmed IO, Helen OO, et al. Production of ethanol from cassava peelings using a developed percolation reactor. J of Sustainable Bioe Systems. 2018; 8: 107-115.
22. Efeovbokhan VE, Egwari L, Alagbe EE, et al. Production of bioethanol from hybrid cassava pulp and peel using microbial and acid hydrolysis. Bio Res. 2019; 14: 2596-2609.
23. Amadi OC, Onyenma NC, Nwagu TN, et al. Total utilization of different parts of wild cocoyam in production of sugar feedstock for bioethanol production; an integrated approach. Bioresource Techn Rep. 2020; 12: 100550.
24. Taherzadeh MJ, Karimi K. Process for ethanol from lignocellulosic materials I: Acid-based hydrolysis processes. Bio Resources. 2007; 2: 472-499.
25. Sun Y, Cheng J. Hydrolysis of lignocellulosic materials for ethanol production: A review. Bioresource Technol. 2002; 83: 1-11.
26. Braide W, Oji IO, Adeleye SA, et al. Comparative study of bioethanol production from agricultural wastes by Zymomonas mobilis and Saccharomyces cerevisiae. In J of Appl Microb Biotec Re. 2018; 6: 50-60.
27. Lenihan P, Orozco A, O'Neill E, et al. Dilute acid hydrolysis of lignocellulosic biomass. Chem Eng J. 2010; 156: 395-403.
28. Abdul ANS, Whitney JP. Differential behaviour of the dinitrosalicylic acid DNS reagent towards mono- and di-saccharide sugars. Biomass Bioenergy. 2011; 35: 4748-4750.